Showa Univ J Med Sci 29(1), 51～67, March 2017

Original

Nasal Septum Morphology in Unilateral and Bilateral Cleft Lip and Palate Determined by 3D Cephalometry

Sachiko YAMAYA[1)], Yuki SATO YAMAMOTO*[1)], Kenji SEKI[2)]
and Koutaro MAKI[1)]

Abstract : We examined vomer morphology using 3-dimensional (3D) analysis and investigated the influence of the surrounding sutures (clefts) and maxilla on nasal septum (vomer) morphology. We evaluated 60 patients who visited our institution. Patients underwent lateral cephalometry and cone-beam computed tomography (CBCT) upon initial examination. Patients with no significant differences in cranial growth were selected and divided into 3 groups of 20 : the bilateral cleft lip and palate (BCLP), unilateral cleft lip and palate (UCLP), and non-cleft (Control) groups. We investigated vomer and facial morphologies by using 2-dimensional (2D) cephalometry and we also determined vomer morphology by using 3D cephalometry. Results were analyzed using Bonferroni multiple comparison, logistic regression analysis, and factor analysis. Vomer morphology was significantly different between the 3 groups. Sagitally, the vomer shape was a narrow quadrilateral that tapered at one end in the BCLP group, trapezoidal in the Control group, and intermediate, like a parallelogram, in the UCLP group. The vomer width was significantly greater in the BCLP group. ($P < 0.05$). A significant difference was only found in the posterior vomer width between the UCLP and Control groups. The vomer volume was significantly larger in the BCLP group. The volume in the UCLP group was larger than in the Control group, but this was not significant. Factor analysis revealed that vomer morphology could be clearly distinguished between the 3 groups. Cleft-associated differences in the vicinity of the vomer–maxilla (palatine bone) fusion may influence vomer formation and may cause the differences observed in vomer morphology between the 3 groups. This suggests that cleft and maxillary morphologies may affect nasal septum morphology.

Key words : nasal septum, vomer, cleft, 3D, CT

Introduction

The influence of cleft lip and palate (CLP) on nasal septum morphology, particularly the induction of septal curvature, is well established[1-3)]. The work of Zuckerkandl[4)] still remains the defining work for septal morphology, even after 100 years. The simple model described by

[1)] *Department of Orthodontics, Showa University School of Dentistry,* 2-1-1 Kitasenzoku, Ohta-ku, Tokyo 145-8515, Japan.
[2)] *Department of Radiology, Showa University School of Dentistry.*
* To whom corresponding should be addressed.

Zuckerkandl[4] enables coronal viewing of the septum and classifies septal morphology into 3 forms: C, S, or "other" curvatures. Although septal anomalies were further classified by Passow[5] and Ballenger[6] into 12 and 9 types, respectively, the basic concepts remain unchanged. However, we recently reported that the morphology of the vomer close to the palatal plate differed in fetuses with CLP compared with the morphology seen in non-CLP fetuses[7]. This result suggests that septal morphological changes cannot be explained by curvature classifications alone.

The nasal septum is located in the midface and forms part of the nasomaxillary complex. This comprises the perpendicular plate of the ethmoid bone superiorly, the vomer inferiorly, and a permanent nasal septal cartilage in the intermediate region[8]. These components grow differently: the nasal septal cartilage is permanent, the vomer grows through membranous ossification, and the ethmoidal region grows through endochondral ossification. To date, septal morphology has only been evaluated as a whole: no study has either subdivided the septum based on anatomical morphology or investigated its association with surrounding bones. Moreover, most techniques have been limited to 2D analyses[4-8].

In this study, we investigated the impact of the cleft and maxilla on nasal septal morphology (vomer) using three-dimensional (3D) imaging in patients with unilateral CLP (UCLP) and bilateral CLP (BCLP), and compared these to a non-cleft (Control) group.

Material and methods

Subjects

Sixty patients (males, n = 32; females, n = 28) who visited our institution were included in this study (Table 1). The patients were divided into 3 groups: the BCLP, UCLP, and non-cleft (Control) groups. Each group included 20 patients. An initial clinical orthodontic diagnosis was achieved at our orthodontic clinic using a dental cone-beam X-ray CT scanner (CB MercuRay, Hitachi Medico Technology, Tokyo, Japan) (CBCT) and lateral cephalometric X-ray system (KXO-80 TOSHIBA, Tokyo, Japan). The mean age at imaging was 6.52 years (range: 5.50–7.11 years). Patients with uncomplicated CLP and no significant differences in cranial growth ($P = 0.73$), as determined by cephalometric measurement of the sella-nasion (S-N) line, were selected (Table 2). The one-stage method was used for initial rhinocheiloplasty and palatoplasty when patients were 6 and 18 months old, respectively. The push-back method[9] was used for palatoplasty. Alveolar cleft bone grafting was not performed. Patients in the control group were classified as skeletal Class Ⅰ.

This study was performed after gaining approval from the Medical Ethics Committee of Showa University School of Dentistry (approval number 2011–23).

Measurements

Lateral cephalometric X-rays were performed using a cephalometric radiography system. The following parameters were used: 80 kV tube voltage, 320 mA tube current, 0.2 s. Craniomaxillofacial images were acquired using a CBCT. The following parameters were used: 120 kV tube

Table 1. Patient Characteristics

	BCLP	UCLP	Contorol	Total
Patients (n ; Male : Female)	20 (15 : 5)	20 (9 : 11)	20 (9 : 11)	60 (8 : 7)
Mean Age (y ; ±SD)	6.16 (± 0.99)	6.32 (± 0.82)	7.07 (± 0.64)	6.52 (± 0.90)

Table 2. Lateral cephalometric radiographic measurements in the 3 groups

Item	BCLP	UCLP	Control
A. S-N	63.41 (±1.80)	63.87 (± 3.30)	64.32 (±2.61)
B. N-ANS	45.98 (±2.48)	46.89 (± 3.13)	48.60 (±2.55)
C. N-Me	104.19 (±4.86)	106.68 (± 7.06)	109.18 (±4.82)
D. Vomer Height	20.90 (±2.50)	23.35 (± 3.61)	26.26 (±2.69)
E. ∠SN-ANS	85.00 (±3.82)	78.99 (± 3.18)	84.83 (±2.80)
F. ∠SN Pl−Superior edge of vomer	16.5 (±1.90)	15.97 (± 2.95)	17.91 (±1.75)
G. ∠FH P−palatal Pl	4.42 (±2.28)	2.61 (± 1.43)	1.94 (±1.50)
H. ∠FH Pl−anterior border Pl	153.25 (±3.25)	151.03 (± 2.95)	149.42 (±2.83)
I. ∠FH Pl−posterior border Pl	163.66 (±2.39)	139.11 (±10.92)	138.90 (±4.62)
J. ∠FH Pl−alisphenoid Pl	25.47 (±5.16)	27.97 (± 5.29)	24.40 (±4.80)
K. ∠alisphenoid Pl−anterior border Pl	127.71 (±5.13)	122.56 (± 6.09)	125.71 (±5.18)
L. ∠alisphenoid Pl−posterior border Pl	40.85 (±6.06)	64.00 (±14.14)	63.84 (±7.40)

*$P < 0.05$
**$P < 0.01$
Pl : Plane

voltage, 15 mA tube current, 512 slices/scan, 9.6 s acquisition time, ϕ 150 mm acquisition range of the P-mode, and 293 µm voxel size.

We measured vomer and facial morphologies by using 2-dimensional (2D) cephalometry, 4 linear and 8 angular items. We also determined vomer morphology by using 3D cephalometry, 7 linear and volume items.

Morphometry

Maxillofacial morphometry and its relationship to the vomer were evaluated from lateral cephalometric radiographs. Morphology was traced on lateral cephalometric radiographs by a single examiner. Baseline points (Fig. 1-1) were determined as follows. The vomer was roughly square and contacted the maxilla inferiorly and the alisphenoid superiorly. The alisphenoid-pterygopalatine fossa intersection point was designated as the vomer superior edge (#2). The alisphenoid-pterygoid process intersection was designated as the posterosuperior vomer edge (#3).

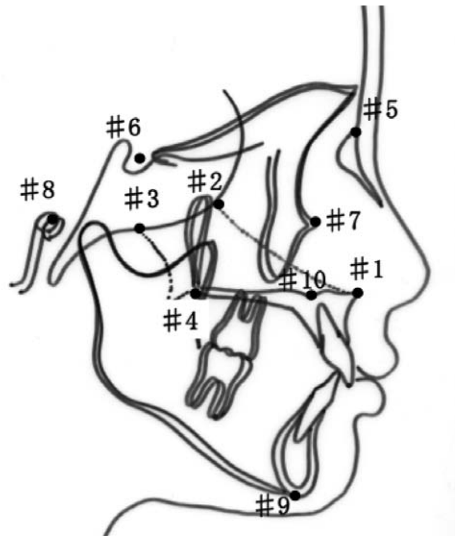

Fig. 1-1. Baseline points were determined according to the Downs-Northwestern method: #1 = anterior nasal spine (ANS); #4 = posterior nasal spine (PNS); #5 = nasion (N); #6 = sella turcica (S); #7 = orbitare (Or); #8 = polion (Po); #9 = menton (Me); and #10 = intersection point of the incisive foramen on the palatal plane (INC). The intersection point of the alisphenoid and pterygopalatine fossa (#2) was determined using the superior edge of the vomer, an established baseline point. The intersection point of the alisphenoid and pterygoid process (#3) was determined using the posterosuperior edge of the vomer, an established baseline point. Point #4 was set as the most posterior point of the lower border of the vomer in the Control and UCLP groups. Because the vomer was not fused with the secondary palate in the BCLP group, point #10 was established as the most posterior point of the lower border.

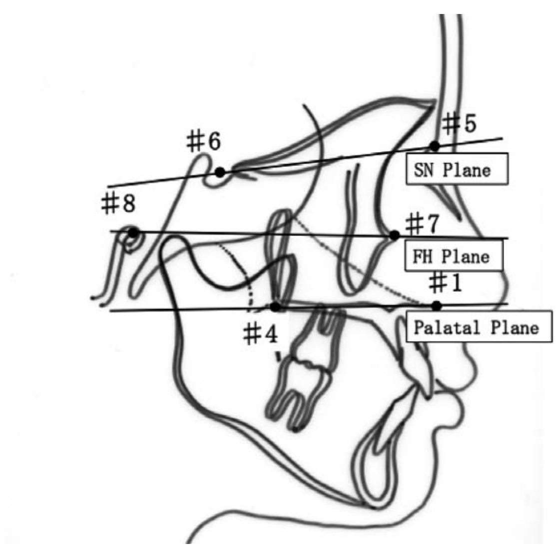

Fig. 1-2. Baseline planes were determined according to the Downs-Northwestern method. SN plane: sella-nasion plane setting the baseline at the cranial base; FH plane: Frankfort horizontal plane; Palatal plane: plane on the maxilla connecting point #1 and point #4.

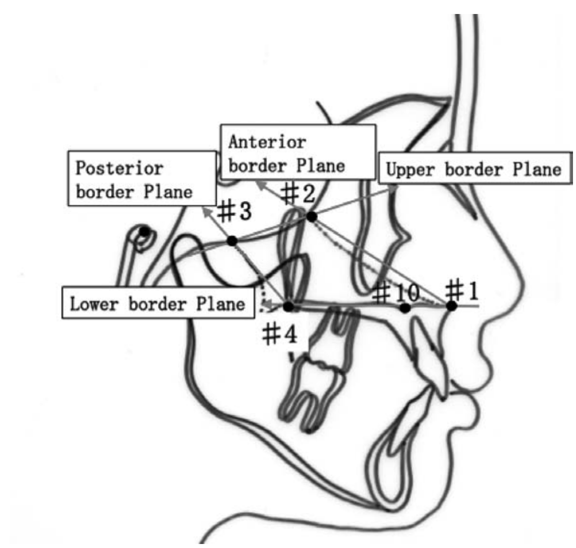

Fig. 1-3. Baseline planes were arbitrarily established for the vomer plane: the anterior border plane, which connects points #1 and #2; the upper border plane, which connects point #2 and #3; the posterior border plane, which connects points #3 and #4 in the control and UCLP groups or points #3 and #10 in the BCLP group; the alisphenoid plane, which connects points #2 and #3.

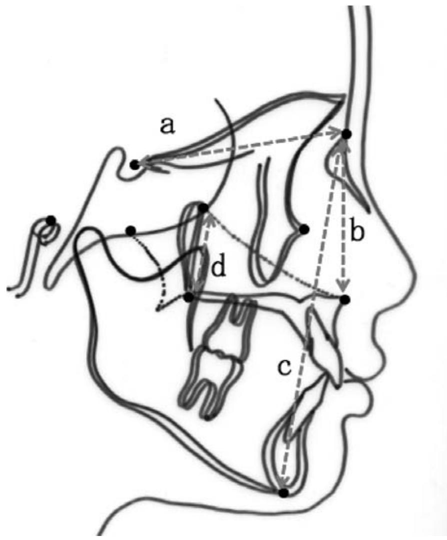

Fig. 2-1. Four items were measured on lateral cephalometric radiographs for facial evaluation. Item A: cranial base length (S-N), item B: upper facial height (N-ANS), item C: facial height (N-Me), and item D: vomer height (distance between points #2 and #4).

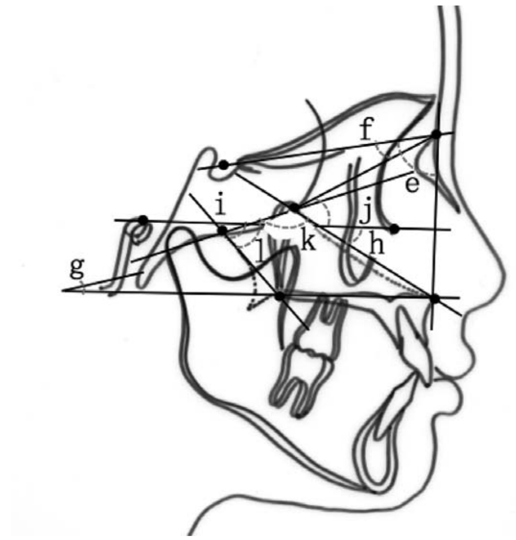

Fig. 2-2. Eight angles were measured on lateral cephalometric radiographs to evaluate vomer and facial morphologies and their positional relationship. Item E: ∠SN Pl–ANS (angle formed by SN plane and ANS); item F: ∠SN Pl–superior edge of the vomer (angle formed by SN plane and point #3); item G: ∠FH Pl–palatal Pl (angle formed by FH and palatal planes); item H: ∠FH Pl–anterior border Pl (angle formed by FH and anterior border planes); item I: ∠FH Pl–posterior border Pl (angle formed by FH and posterior border planes); item J: ∠FH Pl–alisphenoid Pl (angle formed by FH and alisphenoid planes); item K: ∠alisphenoid Pl–anterior border Pl (angle formed by alisphenoid and anterior border planes); and item L: ∠alisphenoid Pl–posterior border Pl (angle formed by alisphenoid and posterior border planes).

These provided baseline points for the upper border of the vomer. Other baseline points were set following the Downs-Northwestern method[10]. Three baseline planes (Fig. 1-2) were also set using the Downs-Northwestern method[10]. Four planes were arbitrarily established for the vomer plane (Fig. 1-3). For facial evaluation, 4 items (Fig. 2-1) were measured following the Downs-Northwestern method[10]. Eight angular items were also established and measured to evaluate vomer and facial morphologies and their positional relationship (Fig. 2-2).

3D vomer morphology and measurements were analyzed using CBCT data. The editor function of 3D shaded surface display (SSD) modeling was used to prepare images of the vomer using CB Works 2.0 (Hitachi Medico Technology). The maximal anatomical clarity threshold was set at 150 based on a preliminary experiment using a dry skull. The vomer was delineated and a 3D object model was prepared for assessment. Four items were defined in the sagittal

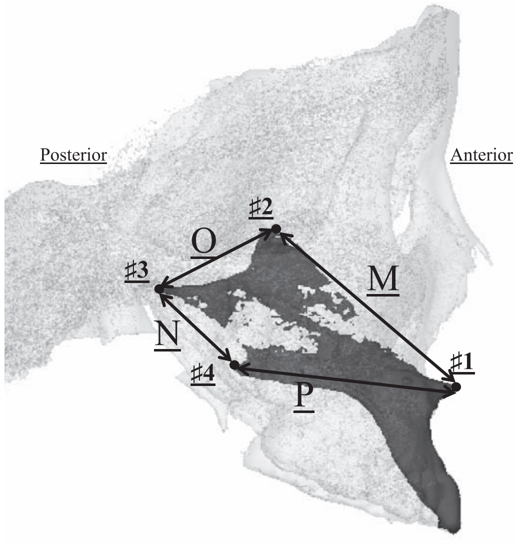

Fig. 3–1. Major axis measurement items established by CBCT in the sagittal view. To measure the major axis of the vomer, 4 items were established in the sagittal view. Item M: anterior-border length, which is the length of the anterior border of the vomer (distance between points #2 and #1) ; item N: posterior-border length, which is the length of the posterior border of the vomer (distance between points #3 and #4 [Control and UCLP groups] or points #3 and #10 [BCLP group]) ; item O: upper-border length, which is the length of contact between the vomer and sphenoid (distance between points #2 and #3) ; and item P: lower-border length, which is the length of contact between the vomer and maxilla [distance between points #1 and #4 (Control and UCLP groups) or points #1 and #10 (BCLP group)].

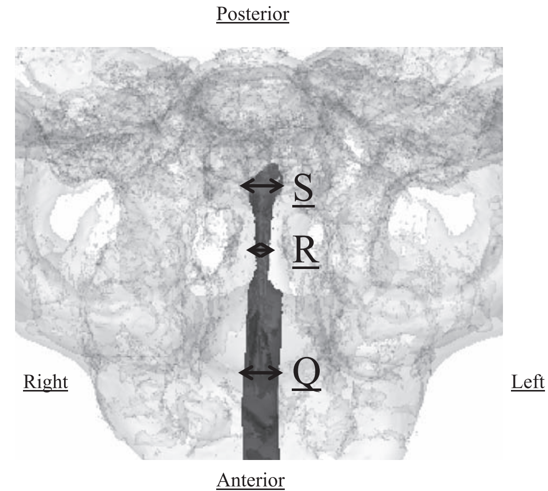

Fig. 3–2. Width measurement items established by CBCT in the horizontal plane. Vomer width was measured by defining 3 items in the horizontal plane (Fig. 3–2). Item Q: anterior-vomer width (width of the most anterior region of the vomer) ; item R: narrow-area width (width of the narrowest region of the vomer) ; and item S: posterior width (width of the alisphenoid).

view to measure the major axis of the vomer (Fig. 3–1). Vomer width was measured by defining 3 items in the horizontal plane (Fig. 3–2). Volume measurements were performed by transferring the CT data to DICOM and importing this into SimPlant® Pro13.0 (Materialise). The palatal plane was set as the baseline in the images and was regarded as the boundary between the vomer and maxilla. The anteroposterior analysis range was then determined. The anatomical morphology of the vomer was determined by selecting sagittal, coronal, and horizontal sections and reconstructing these into a 3D image. The vomer volume was subsequently measured.

Statistical analysis

All measurements were compared using the Bonferroni multiple comparison procedure. A *P*-value < 0.05 was considered statistically significant. The diagnostic performance, or distinguish-

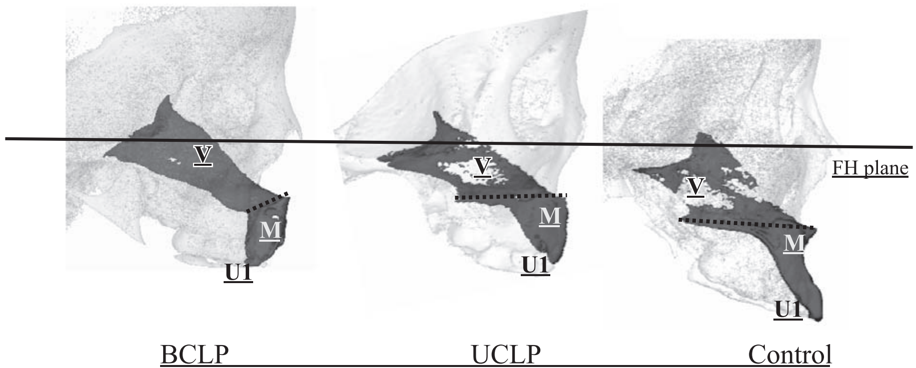

Fig. 4. Typical images of the vomer in the sagittal view in the 3 groups (baseline set at the FH plane). V = vomer, M = maxilla, U1 = upper incisor.

ing ability, of each measurement item was evaluated using receiver operating characteristic area under the curve (ROC AUC) for combinations of the BCLP, UCLP, and Control groups. When necessary, the optimum test combination was determined using a multivariate logistic model, and the Logit value was used as a composite function of the tests; using this function, improvement in differentiation from a single test item was evaluated using ROC AUC. The 3 groups could be clearly identified when the AUC was 1.0 and were distinguishable when the AUC was ≥ 0.8. To investigate the correlation between tests, factor analyses, employing the principle component method and oblique coordinate system conversion, were performed. A factor was considered to be associated with a test item if $\gamma > 0.4$.

Results

Measurements

S-N line lengths measured by cephalometric analysis were not significantly different between the 3 groups ($P = 0.73$). In addition, cranial growth was not significantly affected by the age or sex of the patients in the 3 groups ($P = 0.73$). There was not a large difference in the growth of the cranial maxillary nerve between males and females in the 3 groups, and this did not deviate from the Scammon's curve nerve model (data not shown). These results indicated that there was no significant difference in cranial growth between the 3 groups. The facial height and angle measurements in each of the 3 groups are presented in Table 2. Significant differences were observed in 10 items: items B–I, K and L. The mean ∠FH Pl–alisphenoid plane (item J) was greatest in the UCLP group, followed by the BCLP and Control groups; however, this was not significant ($P = 0.10$).

Vomer morphometry

Figure 4 presents typical CBCT images of the vomer in the sagittal view. The vomer has a quadrilateral shape and its lower border is continuous with the maxilla in each of the 3 groups. However, the shape of the quadrilateral varied among the 3 groups: it was relatively thin, long, and tapered to a short lower border in the BCLP group; it was roughly trapezoidal with a

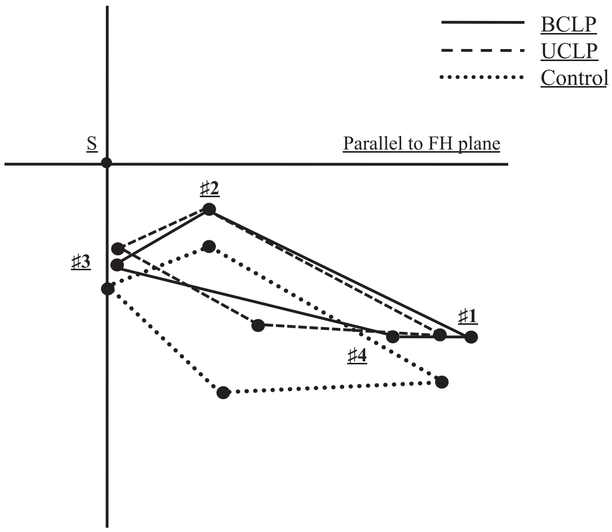

Fig. 5. Superimposition of typical vomer images extracted from cephalometric radiographs for the 3 groups (superimposition on FH plane at S). Baseline points [#1, #2, #3, and #4 (Control and UCLP groups) or #10 (BCLP group)] and baseline planes (palatal, anterior border, posterior border, and alisphenoid planes) were extracted from typical cephalometric radiographs from the 3 groups and superimposed.

longer upper border in the Control group; and in the UCLP group it displayed an intermediate morphology, which approximated to a parallelogram shape with shorter inferior borders compared with those in the Control group. The baseline points (#1, #2, #3, #4, or #10) and planes were extracted from these typical vomer images and superimposed on the Frankfort Horizontal (FH) plane point of S (Fig. 1 #6) to compare the morphology and positional relationship between the 3 groups (Fig. 5). The relationship of the vomer and face differed between the 3 groups. The vomer was located higher in both the BCLP and UCLP groups than in the Control group. In addition, the vertical vomer length was greatest in the Control group and shortest in the BCLP group. Furthermore, the anteroposterior length was greatest in the BCLP group and shortest in the UCLP group. The anteroposterior relationship was similar between the BCLP and Control groups. There were no significant differences between the 3 groups in the vomer superior edge measurements (#2-#3).

Table 3 summarizes the vomer length (sagittal view), width (horizontal view), and volume. Significant differences were observed in 7 items: items M, N, and P-T. The mean upper-border length (item O) was not significantly different between the 3 groups ($P = 0.82$). All vomer width measurements were significantly greater in the BCLP group ($P < 0.05$). Although the anterior (item Q) and narrow-area (item R) widths in the UCLP group were similar to those in the Control group, these differences were not significant. However, there was a significant difference in the posterior width (item S) between the UCLP and Control groups. The vomer volume (item T) was significantly larger ($>$ 2-fold) in the BCLP group and smallest in the Control group; however, the difference between the Control and UCLP groups was not significant.

Logistic regression analysis results

The BCLP and Control groups were differentiated by 10 items (Table 4–1) : vomer height

Table 3. CBCT measurements in the 3 groups

Item		BCLP	UCLP	Control
M.	Anterior-border length	51.11 (±3.30)	45.98 (±2.53)	46.20 (±2.61)
		BCLP–UCLP **		BCLP–Control **
N.	Posterior-border length	47.08 (±5.19)	22.2 (±3.37)	20.87 (±2.19)
		BCLP–UCLP **		BCLP–Control **
O.	Upper-border length	20.70 (±3.58)	20.24 (±2.90)	20.01 (±3.04)
P.	Lower-border length	13.96 (±2.15)	32.74 (±6.62)	39.87 (±2.90)
		BCLP–UCLP **	UCLP–Control **	BCLP–Control **
Q.	Anterior width	4.16 (±1.52)	2.66 (±0.78)	2.84 (±0.78)
		BCLP–UCLP **		BCLP–Control **
R.	Narrow-area width	2.36 (±0.84)	1.44 (±0.54)	1.29 (±0.56)
		BCLP–UCLP **		BCLP–Control **
S.	Posterior width	4.76 (±1.19)	3.83 (±0.70)	2.78 (±0.83)
		BCLP–UCLP *	UCLP–Control **	BCLP–Control **
T.	Volume	1960.75 (±722.97)	841.92 (±235.92)	725.41 (±365.41)
		BCLP–UCLP **		BCLP–Control **

*$P < 0.05$
**$P < 0.01$

Table 4. Logistic regression analysis of the BCLP and Control groups

Item		AUC	*P*-value	Cut off	Sensitivity	Specificity	PP	NP	LR
A.	S-N	0.587	0.3709	63.86	0.625	0.579	0.556	0.647	1.484
B.	N-ANS	0.720	0.0274	46.79	0.625	0.632	0.588	0.667	1.696
C.	N-Me	0.770	0.0123	106.59	0.688	0.684	0.647	0.722	2.177
D.	**Vomer Height**	**0.887**	**0.0026**	**24.00**	**0.813**	**0.789**	**0.765**	**0.833**	**3.859**
E.	∠SN-ANS	0.589	0.2801	84.00	0.563	0.579	0.529	0.611	1.336
F.	∠SN Pl−Superior edge of vomer	0.668	0.1266	17.00	0.688	0.632	0.611	0.706	1.866
G.	∠FH Pl−Palatal Pl	0.793	0.0109	3.00	0.813	0.789	0.765	0.833	3.859
H.	**∠FH Pl−anterior border Pl**	**0.803**	**0.0069**	**28.00**	**0.688**	**0.684**	**0.647**	**0.722**	**2.177**
I.	**∠FH Pl−posterior border Pl**	**1.000**	**0.5229**	**20.00**	**1.000**	**1.000**	**1.000**	**1.000**	**-**
J.	∠FH Pl−alisphenoid Pl	0.579	0.5352	25.00	0.563	0.632	0.563	0.632	1.527
K.	∠alisphenoid Pl−anterior border Pl	0.587	0.6246	127.00	0.563	0.579	0.529	0.611	1.336
L.	**∠alisphenoid Pl−posterior border Pl**	**0.990**	**0.0102**	**48.00**	**0.938**	**0.947**	**0.938**	**0.947**	**17.813**
M.	**Anterior-border length**	**0.918**	**0.0025**	**48.60**	**0.813**	**0.789**	**0.765**	**0.833**	**3.859**
N.	**Posterior-border length**	**1.000**	**0.5483**	**41.31**	**1.000**	**1.000**	**1.000**	**1.000**	**-**
O.	Upper-border length	0.581	0.3673	21.06	0.500	0.526	0.471	0.556	1.056
P.	**Lower-border length**	**1.000**	**0.5600**	**18.10**	**1.000**	**1.000**	**1.000**	**1.000**	**-**
Q.	Anterior width	0.738	0.0133	3.15	0.688	0.632	0.611	0.706	1.866
R.	**Narrow-area width**	**0.849**	**0.0026**	**1.60**	**0.750**	**0.737**	**0.706**	**0.778**	**2.850**
S.	**Posterior width**	**0.941**	**0.0021**	**3.78**	**0.813**	**0.789**	**0.765**	**0.833**	**3.859**
T.	**Volume**	**0.954**	**0.0298**	**1071.66**	**0.813**	**0.789**	**0.765**	**0.833**	**3.859**

Pl : plane, AUC : area under the curve, PP : predicted probability, NP : negative probability, and LR ; likelihood ratio. Data in bold represent an AUC ≧ 0.8.

(item D ; AUC = 0.8), ∠FH Pl–anterior border plane (item H ; AUC = 0.8), ∠FH Pl–posterior border plane (item I ; AUC = 1.0), ∠alisphenoid Pl–posterior border plane (item L ; AUC = 0.9), anterior-border length (item M ; AUC = 0.9), posterior-border length (item N ; AUC = 1.0), lower-border length (item P ; AUC = 1.0), narrow-area width (item R ; AUC = 0.8), posterior width (item S ; AUC = 0.9), and volume (item T ; AUC = 0.9). The UCLP and Control groups were differentiated by 3 items (Table 4–2) : the ∠SN–ANS (item E ; AUC ≥ 0.9), lower-border length (item P ; AUC ≥ 0.8), and posterior width (item S ; AUC ≥ 0.8). The BCLP and UCLP groups were differentiated by 6 items (Table 4–3) : ∠FH plane–posterior border plane (item I ; AUC = 1.0), ∠alisphenoid Pl–posterior border plane (item L ; AUC = 0.9), anterior-border length (item M ; AUC = 0.9), posterior-border length (item N ; AUC = 1.0), lower-border length (item P ; AUC = 0.9), and volume (item T ; AUC ≥ 0.8). Taken together, these results showed that the 3 groups could be differentiated by the following combinations : posterior width (item S) and ∠SN–ANS (item E ; Fig. 6.1) ; lower-border length (item P) and posterior-border length (item N ; Fig. 6.2) ; and ∠FH Pl–posterior border Pl (item I) and posterior-border length (item N ; Fig. 6–3).

Factor analysis results

As per the Eigenvalue variation in the screen test, 4 factors were necessary to distinguish between the 3 groups. We extracted 2 factors based on the correlation between the factors and constituent items (Table 5). These factors were not correlated ($\gamma = 0.262$), and the 3 groups were associated with independent factors. The BCLP ($\gamma = 0.9$) and Control ($\gamma = -0.7$) groups had opposing correlations with Factor 1, suggesting that these 2 groups can be characterized by this factor. Eleven items were associated with Factor 1 : we found positive correlations for items M, N, Q-T and inverse correlations for items B, H, I, L, and P (Fig. 7). The BCLP ($\gamma = 0.455$) and UCLP ($\gamma = -0.776$) groups had opposing correlations with Factor 2, suggesting that these 2 groups were characterized by this factor. In total, 7 items were associated with Factor 2 : positive correlations were found for items E, M, N, Q, R, and T, and an inverse correlation was found for item I (Fig. 7). The BCLP ($\gamma = 0.455$) and Control ($\gamma = 0.327$) groups had similar results for Factor 2, suggesting that these 2 groups possessed similar properties with regard to this factor.

Discussion

The upper region of the vomer is connected to the cranial base (alisphenoid). Our study demonstrated that no significant differences existed in the upper-border length, in the vicinity of vomer-sphenoid fusion, or in the oblique angle in the 3 groups analyzed, and that these had no correlations with vomer morphology. Wang *et al*[11] separated circumaxillary sutures using an orthodontic device and investigated the resulting effects. They found that the effects decreased as the distance from the maxilla increased, and that there were almost no effects near the cranial base. Jeffery *et al*[12] reported that tarsier skulls do not adequately reflect this concept. Our study suggested that clefts only reach the cranial base at the point where the superior edge of

Table 5. Logistic regression analysis of the UCLP and Control groups

Item		AUC	*P*-value	Cut off	Sensitivity	Specificity	PP	NP	LR
A.	S-N	0.526	0.6332	64.56	0.500	0.474	0.474	0.500	0.950
B.	N-ANS	0.662	0.1174	46.65	0.611	0.632	0.611	0.632	1.659
C.	N-Me	0.621	0.2370	107.87	0.611	0.632	0.611	0.632	1.659
D.	Vomer Height	0.703	0.7838	24.50	0.667	0.737	0.706	0.700	2.533
E.	**∠SN-ANS**	**0.901**	**0.0027**	**82.00**	**0.889**	**0.842**	**0.842**	**0.889**	**5.630**
F.	∠SN Pl−Superior edge of vomer	0.724	0.0307	16.50	0.667	0.684	0.667	0.684	2.111
G.	∠FH Pl−Palatal Pl	0.655	0.2751	2.20	0.611	0.684	0.647	0.650	1.935
H.	∠FH Pl−anterior border Pl	0.645	0.1056	29.00	0.500	0.579	0.529	0.550	1.188
I.	∠FH Pl−posterior border Pl	0.545	0.9351	41.00	0.556	0.526	0.526	0.556	1.173
J.	∠FH Pl−alisphenoid Pl	0.716	0.0521	25.00	0.722	0.632	0.650	0.706	1.960
K.	∠alisphenoid Pl−anterior border Pl	0.611	0.2145	123.00	0.611	0.632	0.611	0.632	1.659
L.	∠alisphenoid Pl−posterior border Pl	0.550	0.5461	66.00	0.556	0.526	0.526	0.556	1.173
M.	Anterior-border length	0.534	0.9171	46.36	0.500	0.526	0.500	0.526	1.056
N.	Posterior-border length	0.572	0.1356	21.12	0.500	0.474	0.474	0.500	0.950
O.	Upper-border length	0.504	0.7405	20.34	0.444	0.421	0.421	0.444	0.768
P.	**Lower-border length**	**0.865**	**0.0031**	**36.54**	**0.778**	**0.789**	**0.778**	**0.789**	**3.694**
Q.	Anterior width	0.547	0.4420	2.62	0.500	0.526	0.500	0.526	1.056
R.	Narrow-area width	0.583	0.4421	1.40	0.500	0.526	0.500	0.526	1.056
S.	**Posterior width**	**0.811**	**0.0035**	**3.55**	**0.778**	**0.737**	**0.737**	**0.778**	**2.956**
T.	Volume	0.608	0.2025	800.00	0.611	0.632	0.611	0.632	1.659

Pl : plane, AUC : area under the curve, PP : predicted probability, NP : negative probability, and LR ; likelihood ratio. Data in bold represent an AUC ≧ 0.8.

the vomer fuses to the posterior portion of the cranial base.

Visual morphological differences in the vomer were found between the 3 groups. The vomer was a thin, long, tapered parallelogram in the BCLP group and trapezoidal in the Control group. These differences might be attributed to posterior morphological differences of the inferior border. In complete BCLP, there was no fusion with the secondary palatal plate, excluding the premaxilla, and the most posteroinferior vomer border remained close to the incisive suture (#10) on the anterior side. Therefore, vomer growth might not have been directed toward the posteroinferior direction and might have been concentrated in the anterior region. In the Control group, the fusion range reached the posterior nasal spine (#4), suggesting that bone continuity (fusion) was sufficient to direct vomer growth posteroinferiorly. In complete UCLP, unilateral fusion with the secondary palatal plate was observed, although the fusion range (lower-border length) was significantly shorter compared with that in the Control group and significantly longer compared with that in the BCLP group. This suggests that the vomer in the UCLP group has an intermediate morphology between those in the BCLP and Control groups. The short upper dental arch length reported by Ye *et al*[13] supports this.

We expected a positive correlation between the vomer–palatine bone fusion length and vertical vomer height with a significantly greater vomer height in the Control group. However,

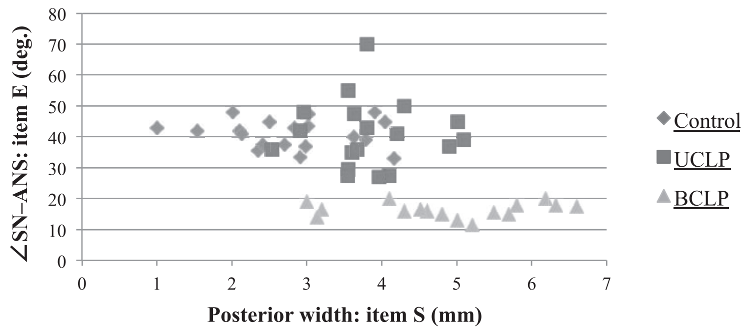

Fig. 6-1. Plot showing the lower-border length (item P) versus the posterior-vomer width (item S) in the 3 groups. Confirmation of data accumulation in each group showed apparent differences in the data collected from the BCLP and Control groups, indicating that these 2 groups could be distinguished from each other on the basis of these results.

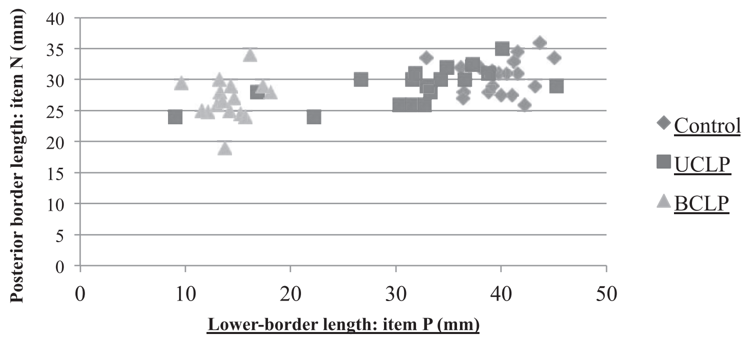

Fig. 6-2. Plot showing the lower-border length (item P) and ∠SN–ANS (item E) in the 3 groups. Data accumulation in each group was confirmed, and showed that the data clustered in individual groups. There were apparent differences between the BCLP and Control groups. The UCLP and the control groups could be distinguished from each other although the UCLP group data were intermediate and relatively scattered.

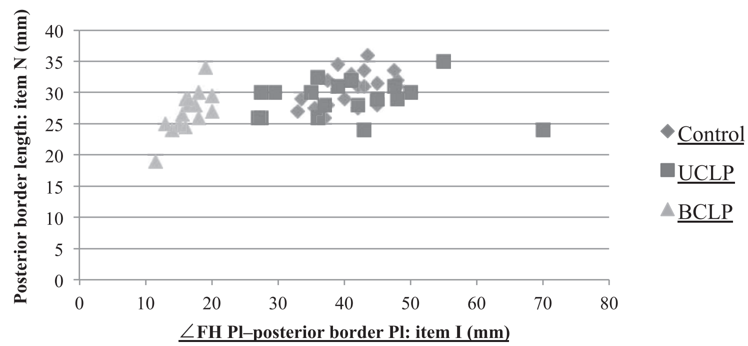

Fig. 6-3. Plot showing the lower-border length (item P) and posterior-border length (item N) in the 3 groups. Data accumulation in each group was confirmed. The data clustered in individual groups and the 3 groups could be distinguished. The data were apparently different between the BCLP and Control groups, whereas those of the UCLP group were intermediate and relatively scattered.

no correlation was observed between these items or between facial and vomer height. Facial-height stunting is associated with CLP, and there are reports of narrow upper dental arches, low posterior upper facial and midface heights resulting from the effects of the push-back method[14]. Despite this, palatal repair has been reported to have no detrimental effects on either the downward displacement of the basal maxilla or palatal remodeling in cases with UCLP[15]. The BCLP group in our study could readily be distinguished from the Control group, but not the UCLP group, based on vomer height. Associations with the 2 factors were also weak. This suggests that vomer height is strongly influenced by cleft type and surgery.

Vomer width differed markedly among the groups but was significantly thicker in the BCLP group. The vomer foot plate is defective in CLP fetuses[7], being round and thick, suggesting congenital vomerial growth differences. Conversely, because the palatine-bone lining (base) is absent and the anterior-teeth occlusal force has to be supported by the vomer alone, its width

Table 6. Logistic regression analysis of the BCLP and UCLP groups

Item		AUC	*P*-value	Cut off	Sensitivity	Specificity	PP	NP	LR
A.	S-N	0.528	0.7970	63.72	0.563	0.556	0.529	0.588	1.266
B.	N-ANS	0.540	0.5159	46.32	0.563	0.556	0.529	0.588	1.266
C.	N-Me	0.595	0.2905	104.68	0.625	0.611	0.588	0.647	1.607
D.	Vomer Height	0.679	0.1059	22.00	0.688	0.611	0.611	0.688	1.768
E.	∠SN-ANS	0.797	0.0081	81.00	0.750	0.722	0.706	0.765	2.700
F.	∠SN Pl−Superior edge of vomer	0.554	0.4134	16.50	0.438	0.611	0.500	0.550	1.125
G.	∠FH Pl−Palatal Pl	0.358	0.4850	3.00	0.375	0.389	0.353	0.412	0.614
H.	∠FH Pl−anterior border Pl	0.696	0.0687	28.00	0.688	0.611	0.611	0.688	1.768
I.	**∠FH Pl−posterior border Pl**	**1.000**	**0.3609**	**20.00**	**1.000**	**1.000**	**1.000**	**1.000**	**-**
J.	∠FH Pl−alisphenoid Pl	0.611	0.1761	25.00	0.563	0.611	0.563	0.611	1.446
K.	∠alisphenoid Pl−anterior border Pl	0.682	0.0600	128.00	0.563	0.611	0.563	0.611	1.446
L.	**∠alisphenoid Pl−posterior border Pl**	**0.929**	**0.0054**	**48.00**	**0.938**	**0.889**	**0.882**	**0.941**	**8.438**
M.	**Anterior-border length**	**0.927**	**0.0028**	**48.53**	**0.875**	**0.889**	**0.875**	**0.889**	**7.875**
N.	**Posterior-border length**	**1.000**	**0.5064**	**41.31**	**1.000**	**1.000**	**1.000**	**1.000**	**-**
O.	Upper-border length	0.566	0.5170	21.02	0.563	0.556	0.529	0.588	1.266
P.	**Lower-border length**	**0.938**	**0.0088**	**16.80**	**0.875**	**0.889**	**0.875**	**0.889**	**7.875**
Q.	Anterior width	0.760	0.0101	3.15	0.688	0.667	0.647	0.706	2.063
R.	Narrow-area width	0.821	0.0050	1.81	0.750	0.722	0.706	0.765	2.700
S.	Posterior width	0.774	0.0099	4.20	0.750	0.722	0.706	0.765	2.700
T.	**Volume**	**0.958**	**0.0114**	**1081.99**	**0.813**	**0.833**	**0.813**	**0.833**	**4.875**

Pl : plane, AUC : area under the curve, PP : predicted probability, NP : negative probability, and LR ; likelihood ratio. Data in bold represent an AUC ≧ 0.8.

might gradually increase as the bone thickens in BCLP. In UCLP, this development might be less marked because the region was partially connected to the secondary palate. This assumption is supported by our finding that vomer width and volume were inversely correlated with the lower-border length.

Anteroposteriorly, the vomer was located more posteriorly in the UCLP group than in the other groups. Although insignificant, with regard to the BCLP and Control groups, the vomerial upper and lower regions were located posteriorly and anteriorly, respectively. Vertically, the vomer was shortest and lowest in the BCLP group based on midface N-ANS and vomer height. The Control group had a high vertical height of the vomer, and BCLP group was short, and UCLP group out that it has the height of its middle. We considered that the vertical height of the vomer is proportional to Facial height. The lower-border (palatal) plane was more oblique in the UCLP and BCLP groups, with an anteroposterior difference in the vomerial vertical position. Iwasaki *et al* [16] reported an anterior ANS in a non-cleft group and a superoposterior inclination of the palatal plane in the cleft groups. However, when the cleft group was divided into cases with and without palatoplasty, there was no significant difference. Therefore, they concluded that palatoplasty does not cause palatal plane inclination and that this must be a natural tendency. Our results concurred, but it cannot be concluded that inclination is a natural effect

Table 7. Correlations between Factors 1 and 2 in the 3 groups

Item		Factor 1	Factor 2
BCLP		**0.900**	**0.455**
UCLP		−0.163	**−0.776**
Control		**−0.723**	0.327
A.	S-N	−0.196	0.029
B.	N-ANS	**−0.427**	−0.038
C.	N-Me	−0.385	−0.052
D.	Vomer Height	−0.346	−0.068
E.	∠SN-ANS	0.071	**0.839**
F.	∠SN Pl−Superior edge of vomer	−0.141	0.026
G.	∠FH Pl−Palatal Pl	0.363	−0.111
H.	∠FH Pl−anterior border Pl	**−0.523**	−0.08
I.	∠FH Pl−posterior border Pl	**−0.847**	**−0.446**
J.	∠FH Pl−alisphenoid Pl	−0.064	−0.205
K.	∠alisphenoid Pl−anterior border Pl	0.24	0.222
L.	∠alisphenoid Pl−posterior border Pl	**−0.732**	−0.322
M.	Anterior-border length	**0.708**	**0.589**
N.	Posterior-border length	**0.881**	**0.45**
O.	Upper-border length	0.147	0.122
P.	Lower-border length	**−0.864**	−0.119
Q.	Anterior width	**0.466**	**0.488**
R.	Narrow-area width	**0.683**	**0.434**
S.	Posterior width	**0.711**	0.044
T.	Volume	**0.766**	**0.42**

Pl : plane
+ : positive correlation
− : inverse correlation
Data in bold represent a γ-value > 0.4.

of the cleft itself, because our factor analysis did not show any factor correlation with cleft type. However, it was apparent that the vomer–palatine bone fusion influenced vertical growth, and we consider that this is likely a result of the combined effects of cleft type and surgery.

We found that the vomer position was more anterior in the BCLP group than in the Control group and that its vertical position was the lowest in the BCLP group. Anteroinferior protrusion of the premaxilla is often observed in BCLP cases. In this study, we assumed that the anteroinferior protrusion of the premaxilla anterior to the vomer was an intraoral symptom caused by the low, posterior position of the palatine bone surrounding the premaxilla. In the BCLP group, restricted vertical vomer growth was observed, whereas anteroposterior growth was not restricted in the Control group. We assumed that the palatine bone lost its forward driving-force because of the lack of continuity with the vomer, resulting in anteroposterior hypogrowth. Sarnat[17] stated that the nasal septum is the facial growth-center and discussed various experimental surgical methods. Maxillofacial growth, particularly maxillary growth, is a multifac-

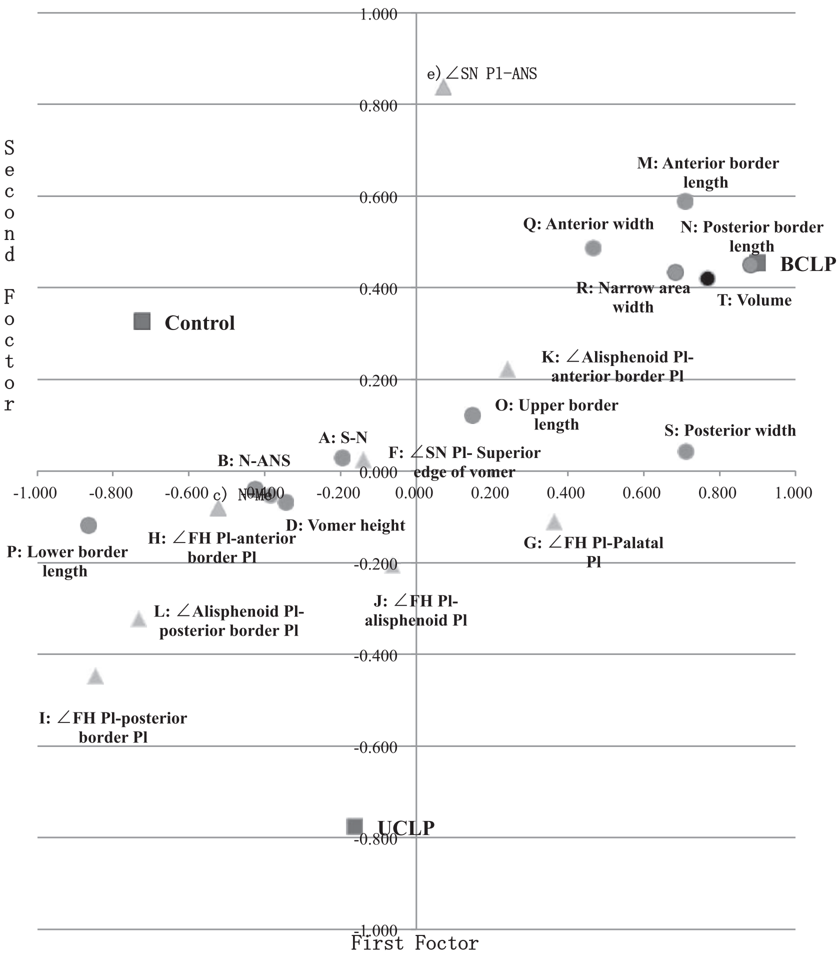

Fig. 7. Factor correlation diagram. Correlation coefficients obtained by correlating the measurement items listed in Table 5 with Factors 1 and 2 were plotted to visualize the correlation of factor structure. The influence of the 2 factors was strongest when the results were close to 1.0 or −1.0. The BCLP and Control groups had opposing correlations, with the boundary set at Factor 1, suggesting that Factor 1 discriminates between BCLP and Control. The BCLP and UCLP groups also had opposing correlations with the boundary set at Factor 2, suggesting that Factor 2 discriminates between BCLP and UCLP. The measurement items that are more strongly associated with discriminating between groups appear close to the BCLP, UCLP, and Control group plots presented on the graph. The 3 groups are clearly distinguishable.

torial process involving sutural growth, bone remodeling, and muscular interaction[18–21]. Many researchers now consider the nasal septum theory as the only logical interpretation; growth of a jaw face by classification of the two-dimensional nasal septum form. Although this study cannot confirm this, our results suggest that the vomer and maxilla are associated with growth.

Regression and factor analyses clearly differentiated vomer morphology between the 3 groups, and 2 key factors were indicated: Factor 1 discriminated between and characterized the BCLP and Control groups, and Factor 2 characterized the BCLP and UCLP groups. The UCLP and

Control groups had the same positive tendency with Factor 1. Further, the lower border presented a strong inverse correlation, suggesting that Factor 1 represents a suture between the secondary palate and vomer. The BCLP and Control groups revealed the same positive tendency with Factor 2. Considering the strong correlation with the primary palatal region (premaxilla/incisive bone; items E, M, and Q), this factor probably represents the bilateral incisive sutures connecting the primary and secondary palates. However, the BCLP and UCLP groups revealed opposing correlations, whereas the BCLP and Control groups revealed a similar tendency. This suggests that Factor 2 represents a growth factor and growth vector transmitted to the primary palate (incisive bone) through the suture, indicating that growth direction might have been symmetrical in both of these groups. These 2 factors were influential, independent, and non-correlated. Although patients in both the UCLP and BCLP groups underwent cheiloplasty and palatoplasty, correlation of morphometric items with these factors might be attributed to the cleft itself, rather than surgery, because the factors were independent.

Conclusion

Our results suggest that the maxilla and clefts are closely involved in nasal-septum morphology, particularly of the vomer, and that morphological growth varied according to the site and extent of the cleft.

Conflict of interest disclosure

None of the authors have any conflicts of interests to declare.

RReferences

1) Harvold E. Cleft lip and palate: Morphologic studies of the facial skeleton. *Am J Orthod*. 1954;**40**:493–506.
2) Latham RA. The pathogenesis of the skeletal deformity associated with unilateral cleft lip and palate. *Cleft Palate J*. 1969;**6**:404–414.
3) Ross RB, Johnston MC. Cleft Lip and Palate. Baltimore: Williams & Wilkins; 1972.
4) Zuckerkandl E. Normale und pathologische Anatomie der Nasenhohle und ihrer pneumatischen Anhange. Vol. 1, 2nd ed. Vienna, Austria: Wilhelm Braumuller; 1893.
5) Dental Journal of Iwate Medical University. 1987;**12(3)**:261–276.
6) Ballenger WL. Diseases of the nose, throat and ear: medical and surgical. 4th ed. Philadelphia: Lea & Febiger; 1914.
7) Hansen L, Nolting D, Holm G, *et al*. Abnormal vomer development in human fetuses with isolated cleft palate. *Cleft Palate Craniofac J*. 2004;**41**:470–473.
8) Scott JH, Dixon AD. Anatomy for Students of dentistry. Edinburgh: Livingstone; 1959.
9) Cronin TD. Method of preventing raw area on nasal surface of soft palate in push-back surgery. *Plast Reconstr Surg (1946)*. 1957;**20**:474–484.
10) Downs WB. Variations in facial relationships; their significance in treatment and prognosis. *Am J Orthod*. 1948;**34**:812–840.
11) Wang YC, Chang PM, Liou EJ. Opening of circumaxillary sutures by alternate rapid maxillary expansions and constrictions. *Angle Orthod*. 2009;**79**:230–234.

12) Jeffery N, Davies K, Kockenberger W, *et al*. Craniofacial growth in fetal Tarsius bancanus: brains, eyes and nasal septa. *J Anat*. 2007;**210**:703–722.

13) Ye B, Ruan C, Hu J, *et al*. A comparative study on dental-arch morphology in adult unoperated and operated cleft palate patients. *J Craniofac Surg*. 2010;**21**:811–815.

14) Andoh Y, Ishikawa H, Nakamura S. A study of structural deformities on nasomaxillary complex in unilateral cleft lip and palate. *J Jpn Cleft Palate Assoc*. 1994;**19**:222–240.

15) Liao YF, Mars M. Long-term effects of palate repair on craniofacial morphology in patients with unilateral cleft lip and palate. *Cleft Palate Craniofac J*. 2005;**42**:594–600.

16) Iwasaki H, Kudo M, Yamamoto Y. Influences of palatoplasty by the push-back procedure on craniofacial morphology and growth. *J Craniomaxillofac Surg*. 2012;**40**:638–646.

17) Sarnat BG. The postnatal maxillary-nasal-orbital complex:some considerations in experimental surgery, In *McNamara JA Jr ed. Factors Affecting the Growth of the Midface : proceedings of a sponsored symposium honoring Professor Robert E. Moyers, held February 6 and 7, 1976, in Ann Arbor, Michigan*. Ann Arbor, Michigan: Center for Human Growth and Development, University of Michigan; 1976. pp101–129. (Craniofacial growth series; monograph no. 6).

18) Aizenbud D, Morrill LR, Schendel SA. Midfacial trauma and facial growth : a longitudinal case study of monozygotic twins. *Am J Orthod Dentofacial Orthop*. 2010;**138**:641–648.

19) Holton NE, Franciscus RG, Marshall SD, *et al*. Nasal septal and premaxillary developmental integration : implications for facial reduction in Homo. *Anat Rec* (*Hoboken*). 2011;**294**:68–78.

20) Mladina R. The role of maxillar morphology in the development of pathological septal deformities. *Rhinology*. 1987;**25**:199–205.

21) Wong KK, Filatov S, Kibblewhite DJ. Septoplasty retards midfacial growth in a rabbit model. *Laryngoscope*. 2010;**120**:450–453.

[Received April 11, 2016 : Accepted December 5, 2016]